

# $\gamma$ -Tubulin Ring Complexes and EB1 play antagonistic roles in microtubule dynamics and spindle positioning

Anaïs Bouissou<sup>1</sup>, Christel Vérollet<sup>2</sup>, H  l  ne de Forges<sup>3</sup>, Laurence Haren<sup>1</sup>, Yohanns Bella  che<sup>4</sup>, Franck Perez<sup>3</sup>, Andreas Merdes<sup>1</sup> & Brigitte Raynaud-Messina<sup>1,\*</sup>

## Abstract

$\gamma$ -Tubulin is critical for microtubule (MT) assembly and organization. In metazoa, this protein acts in multiprotein complexes called  $\gamma$ -Tubulin Ring Complexes ( $\gamma$ -TuRCs). While the subunits that constitute  $\gamma$ -Tubulin Small Complexes ( $\gamma$ -TuSCs), the core of the MT nucleation machinery, are essential, mutation of  $\gamma$ -TuRC-specific proteins in *Drosophila* causes sterility and morphological abnormalities via hitherto unidentified mechanisms. Here, we demonstrate a role of  $\gamma$ -TuRCs in controlling spindle orientation independent of MT nucleation activity, both in cultured cells and *in vivo*, and examine a potential function for  $\gamma$ -TuRCs on astral MTs.  $\gamma$ -TuRCs locate along the length of astral MTs, and depletion of  $\gamma$ -TuRC-specific proteins increases MT dynamics and causes the plus-end tracking protein EB1 to redistribute along MTs. Moreover, suppression of MT dynamics through drug treatment or EB1 down-regulation rescues spindle orientation defects induced by  $\gamma$ -TuRC depletion. Therefore, we propose a role for  $\gamma$ -TuRCs in regulating spindle positioning by controlling the stability of astral MTs.

**Keywords** gamma-tubulin complexes; microtubule dynamics; mitosis; spindle orientation

**Subject Categories** Cell Adhesion, Polarity & Cytoskeleton; Cell Cycle  
**DOI** 10.1002/embj.201385967 | Received 12 June 2013 | Revised 2 October 2013 | Accepted 16 October 2013

**EMBO Journal (2014) 33, 114–128**

## Introduction

$\gamma$ -Tubulin is essential for initiation and regulation of MT assembly. In metazoan organisms, this protein acts in highly ordered multiprotein complexes called  $\gamma$ -TuRCs for  $\gamma$ -Tubulin Ring Complexes

(Moritz *et al*, 1995; Raynaud-Messina & Merdes, 2007). The core subunits of these complexes are the  $\gamma$ -TuSCs ( $\gamma$ -Tubulin Small Complexes), composed of  $\gamma$ -tubulin and two other proteins sharing conserved domains identified as ‘grip motifs’ (Dgrip84 and Dgrip91 in *Drosophila*; GCP2 and GCP3 in humans). The  $\gamma$ -TuRCs are formed of  $\gamma$ -TuSCs associated with three additional grip-motif-polypeptides (Dgrip75, Dgrip128 and Dgrip163 in *Drosophila*; GCP4, GCP5 and GCP6 in humans) (Oegema *et al*, 1999; Teixido-Travesa *et al*, 2012). Other  $\gamma$ -TuRC components unrelated to ‘grip-GCP’ proteins, such as Nedd1 or Mozart proteins, have been described (Haren *et al*, 2006; Luders *et al*, 2006; Choi *et al*, 2010; Hutchins *et al*, 2010; Teixido-Travesa *et al*, 2010).  $\gamma$ -Tubulin complexes localize to all identified MT organizing centers and along spindle MTs (Lajoie-Mazenc *et al*, 1994; Raynaud-Messina *et al*, 2004; Luders & Stearns, 2007).

All  $\gamma$ -TuSC subunits are essential (Oakley *et al*, 1990; Horio *et al*, 1991; Sunkel *et al*, 1995; Knop & Schiebel, 1997; Barbosa *et al*, 2000; Vardy & Toda, 2000; Yuba-Kubo *et al*, 2005; Colombie *et al*, 2006). Mutation or loss of  $\gamma$ -TuSC proteins results in the accumulation of cells in mitosis, with defects such as monopolar spindles, abnormal centrosome maturation and aneuploidy. In contrast, mutants in  $\gamma$ -TuRC-specific grip motif proteins are viable in fungi and in *Drosophila* (Fujita *et al*, 2002; Schnorrer *et al*, 2002; Venkatram *et al*, 2004; Anders *et al*, 2006; Verollet *et al*, 2006; Xiong & Oakley, 2009). However, *Drosophila* adults of both sexes are sterile and display a slight increase in lethality after hatching, as well as defects in abdominal morphology and in the thoracic bristle pattern (Verollet *et al*, 2006). In mutant larval neuroblasts, most of the spindles are bipolar although a significant increase in aneuploidy is observed. In cultured *Drosophila* cells, depletion of any  $\gamma$ -TuRC-specific grip-motif protein (Dgrip75, 128 and 163) induces elongated bipolar spindles with  $\gamma$ -tubulin failing to associate with spindle MTs, and weakly accumulating at the poles (Verollet *et al*, 2006). In mammalian cells, depletion of human GCP6 induces stronger phenotypes, with defects in centriole number and a high percentage of monopolar spindles (Bahtz *et al*, 2012). All grip-motif proteins are

1 Centre Biologie du D  veloppement, UMR 5547, CNRS-UPS Toulouse 3, Toulouse Cedex 04, France

2 Institut de Pharmacologie et de Biologie Structurale, UMR 5089, Toulouse Cedex 04, France

3 Institut Curie, CNRS UMR144, Paris Cedex 05, France

4 Institut Curie, CNRS UMR 3215-INSERM U934, Paris Cedex 05, France

\*Corresponding author. Tel: +33 5 61 17 54 72; Fax: +33 5 61 17 59 94; E-mail: brigitte.raynaud@ipbs.fr

critical for the assembly or stability of the  $\gamma$ -TuRCs which constitute the main MT nucleating template (Oegema *et al*, 1999; Verollet *et al*, 2006; Izumi *et al*, 2008; Kollman *et al*, 2011).

Our purpose is to gain further insight into the mechanisms by which  $\gamma$ -TuRC-specific proteins influence developmental processes. As studies in yeasts and *Drosophila* identified mutations in  $\gamma$ -tubulin or in associated proteins that do not strongly affect MT assembly, but induce defects in MT dynamics, we hypothesize that these proteins act in development through functions not exclusively dependent on nucleation (Paluh *et al*, 2000; Fujita *et al*, 2002; Zimmerman & Chang, 2005; Cuschieri *et al*, 2006; Masuda *et al*, 2006; Rogers *et al*, 2008; Bouissou *et al*, 2009; Anders & Sawin, 2011). We performed live analysis of cells depleted of a grip-protein specific of the ring complexes. We show that the  $\gamma$ -TuRCs are involved in spindle positioning both in cell cultures and *in vivo*. Because the proper orientation of the spindles relies on the interactions between the cortex and astral MTs, we studied the potential localization and function of  $\gamma$ -TuRCs on astral MTs. We obtained evidence for a role of  $\gamma$ -TuRCs on the dynamics of astral MTs. Moreover, the disassembly of  $\gamma$ -TuRCs prevented the proper accumulation of EB1 on MTs. Since simultaneous depletion of EB1 and of a  $\gamma$ -TuRC-specific protein reconstituted spindle orientation, we suggest that antagonistic effects between EB1 and the  $\gamma$ -TuRCs govern astral MT behaviour.

## Results

### $\gamma$ -TuRCs participate in spindle positioning

To better understand how  $\gamma$ -TuRCs contribute to proper spindle organization, we first followed mitosis using live-cell imaging in *Drosophila* GFP- $\alpha$ -tubulin-S2 cells depleted of the  $\gamma$ -TuRC-specific protein, Dgrip75. Observation of cells plated on concanavalin A (ConA)-coated coverslips for short periods of time ( $\approx 120$  s) confirmed the phenotypes previously observed by fixed immunofluorescence (IF) microscopy such as long interpolar distances and low internal MT densities (supplementary Fig S1A and B, left panel; Verollet *et al*, 2006). We further observed the presence of astral MTs that were usually longer than in untreated cells (supplementary Fig S1B, middle panel). We did not notice significant modification in their number nor in their anchoring to the poles, suggesting no major problems at astral MT minus ends (supplementary Fig S1B, right panel). Moreover, we quantified the density of astral MTs around the metaphase poles at steady state (supplementary Fig S1C, left panel) and during MT regrowth after cold depolymerisation (supplementary Fig S1C, right panels). Only a subtle delay was observed in Dgrip75-depleted cells compared with control cells (at +15 s), but the number of MTs rapidly became indistinguishable. Altogether, these data show that the nucleation activity at the pole appears comparable in control and Dgrip75-deficient cells. However, overnight imaging of cells on glass coverslips revealed that down-regulation of Dgrip75 led to an increase in the duration of mitosis (1 h  $\pm$  15 min in control versus 1 h 45  $\pm$  25 min in RNAi-treated cells,  $n = 20$ ) and to defects in spindle positioning (Fig 1A and supplementary movie S1). Compared to control spindles, Dgrip75-depleted spindles rotated with angles significantly higher (about twofold), until the final axis of division was reached. Using static GFP- $\alpha$ -tubulin dots outside the MTs as reference points, we verified

that the recorded rotation of the spindles did not result from an overall movement of the cells (supplementary Fig S1D). To acquire additional evidence for a role of  $\gamma$ -TuRCs in spindle positioning, we used a model of 'induced polarity' in S2 cells (Johnston *et al*, 2009; Fig 1B). This system allows the asymmetric cortical distribution of a polarity actor (i.e., Pins<sup>TRP+linker</sup>) in the otherwise unpolarised S2 cells. Briefly, Pins<sup>TRP+linker</sup> was fused in frame to the cell adhesion molecule Echinoid (Ed). Upon Ed-dependent cell clustering induced by shaking, Pins<sup>TRP+linker</sup> was enriched to the site of cell-cell contact. Metaphase spindles of cells expressing Ed alone did not adopt any preferential orientation. In contrast, the fusion Ed-Pins<sup>TRP+linker</sup> resulted in a robust orientation of the spindles. Depletion of Dgrip75 abolished spindle orientation activity of the Ed-Pins<sup>TRP+linker</sup> construction. Similar effects were observed after depletion of Dgrip128, another grip-motif protein specific for  $\gamma$ -TuRCs (supplementary Fig S2A).

To investigate whether the role of  $\gamma$ -TuRCs is conserved in mammalian cells, we studied the role of GCP4, the human ortholog of Dgrip75, in HeLa cells (Fava *et al*, 1999). These cells preferentially orient their spindles parallel to the plane of the coverslips (Toyoshima & Nishida, 2007). GCP4 siRNA treatment did not significantly alter  $\gamma$ -tubulin level but resulted in bipolar spindles with  $\gamma$ -tubulin absent from spindle MTs and faintly staining the poles (Supplemental Fig S4B–D). Under these conditions, metaphase spindles were misoriented compared to controls (Fig 1C and supplementary Fig S1F). The mean angle between the axis of the metaphase spindle and that of the plate surface increased by about 2.5-fold after siRNA treatment (mean angle  $5.5^\circ \pm 0.8$  in control cells compared to  $13^\circ \pm 1.2$  in depleted cells). This effect was specific as it was rescued by the expression of GCP4 resistant to siRNA treatment.

We next tested whether the involvement of the  $\gamma$ -TuRCs in spindle orientation observed in cell cultures has any relevance *in vivo*. As spindle orientation appears crucial in asymmetric divisions, we analyzed spindle orientation during the asymmetric divisions of the third instar larval *Drosophila* neuroblasts. During these divisions, the mitotic spindles are oriented along the polarity axis marked by the basal localization of the Miranda adaptor protein (for a review, see Siller & Doe, 2009). Therefore, we quantified spindle orientation in wild-type and *Dgrip75*<sup>175</sup> mutants, by measuring the angle between the pole-pole axis and a line bisecting the Miranda crescent (Fig 1D). The nonsense *Dgrip75*<sup>175</sup> mutant results in a truncation of the predicted protein in the N-part of the protein, suggesting either null or at least strong allele (Schnorrer *et al*, 2002). While the spindles in *Dgrip75* mutants remained bipolar, they presented a mean angle ( $15^\circ \pm 1.9$ ) relative to the position of Miranda crescent significantly higher than the one observed in wild-type ( $10.8^\circ \pm 1$ ).

Altogether, these data show that in addition to their previously reported role in spindle morphology (Verollet *et al*, 2006),  $\gamma$ -TuRCs are involved in spindle positioning both in cultured cells and during asymmetric divisions of *Drosophila* neuroblasts.

### $\gamma$ -TuRCs localize along astral MTs

Since spindle positioning is controlled by interactions between the astral MTs and the cell cortex (Pearson & Bloom, 2004; Kunda & Baum, 2009), we studied the precise localization of  $\gamma$ -tubulin and associated proteins during mitosis, with a particular focus on astral MTs. We first used *Drosophila* S2R<sup>+</sup> cells because of their spread morphology. In addition to the already described sites of localization

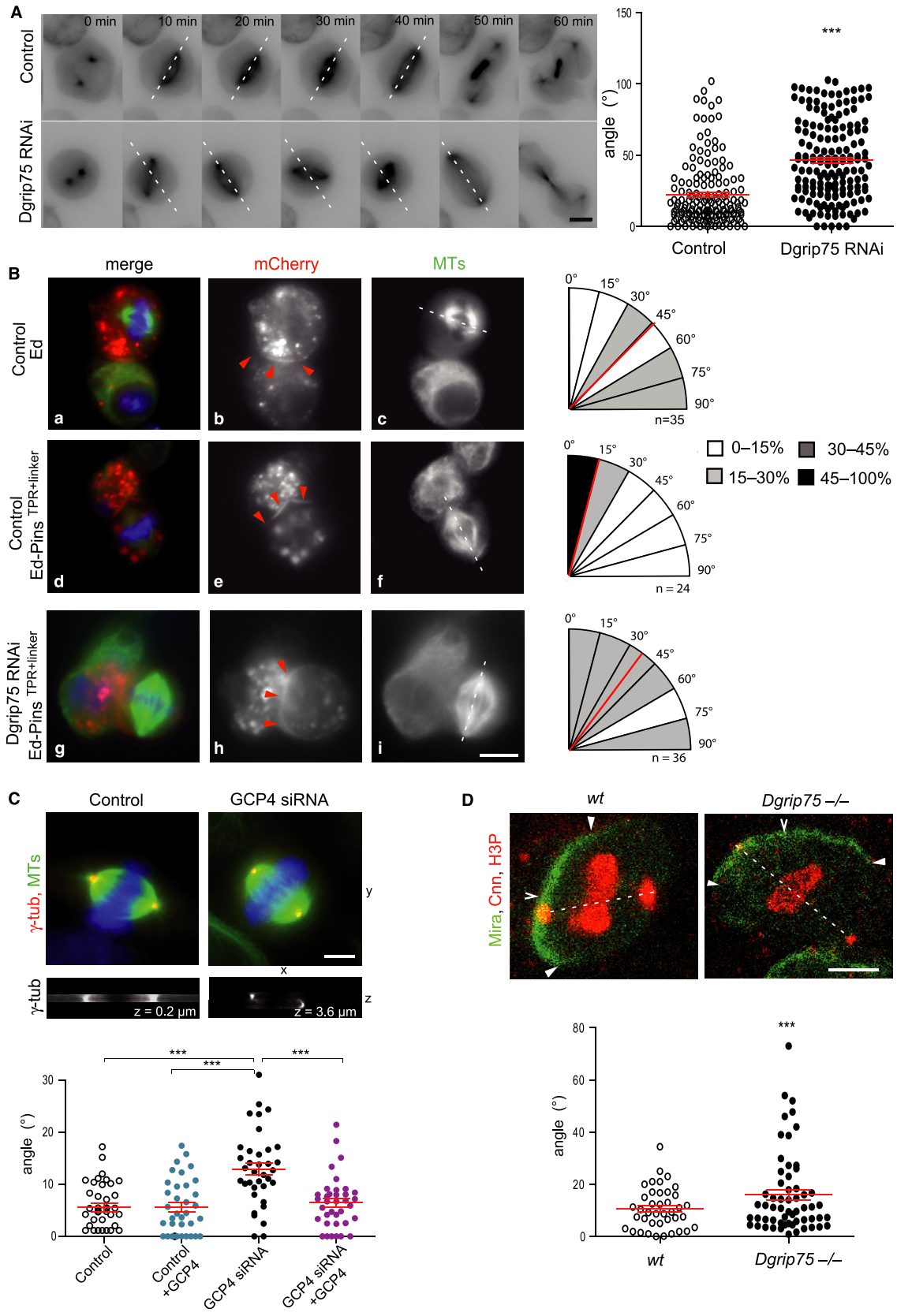


**Figure 1.  $\gamma$ -TuRCs control spindle positioning in *Drosophila* and mammalian cells.**

- A** Defects in spindle positioning after Dgrip75 depletion in S2 cells expressing GFP- $\alpha$ -tubulin. Left panel: Time-lapse sequences of cells plated on glass coverslips, see supplementary movie S1. White dotted lines indicate the anaphase axis. Right panel: Distribution of spindle angle amplitude ( $^{\circ}$ ) from prometaphase to anaphase in control and in Dgrip75-depleted cells ( $n > 110$  cells, 3 independent experiments).
- B** Defects in spindle orientation after Dgrip75 depletion in induced polarity S2 cells. Left panels: Echinoid tagged with mCherry epitope (Ed::mCherry) alone (upper row) or fused with the TRP+linker of Pins (Ed::mCherry-Pins<sup>TRP+linker</sup>) were transfected in control cells (middle row) or in Dgrip75-depleted cells (lower row). Cells were stained for  $\alpha$ -tubulin (green) (c, f, i) and DNA (blue). Merge (a, d, g). Right panels: Spindle angle repartition. Angles represent the values between the vectors perpendicular to the Ed crescents (red arrowheads) and the spindle axes (white dotted lines). Red line: median angle, n: number of measured spindles. The difference between the mean angles of Ed::mCherry-Pins<sup>TRP+linker</sup> and the two other conditions are statistically significant ( $P < 0.001$ , 3 independent experiments).
- C** Defective spindle orientation after GCP4 depletion in HeLa cells. Upper panel: Control or GCP4-depleted cells were immunostained for  $\alpha$ -tubulin (green),  $\gamma$ -tubulin (red) and DNA (blue) and imaged in z (0.2  $\mu$ m-thick sections). Middle panel:  $\gamma$ -Tubulin staining of the cross-section through the two poles of the same cell. Lower panel: Distribution of spindle angles ( $^{\circ}$ ) in control and in GCP4-depleted cells, without or with expression of exogenous GCP4 resistant to siRNA treatment. The values represent the angles between the axis crossing the two poles of metaphase spindles and the coverslip. Two independent experiments with  $\geq 35$  spindles per condition.
- D** Defects in spindle orientation in *Dgrip75*<sup>-/-</sup> neuroblasts. Upper panel: Wild-type (*wt*) and *Dgrip75* mutant (*Dgrip75*<sup>-/-</sup>) neuroblasts of third instar larvae stained with Centrosomin (Cnn: red), phospho-histone H3 (H3P: red) and Miranda (Mira: green, white arrowheads). Lower panel: Distribution of spindle angle ( $^{\circ}$ ) relative to Miranda crescent. Two independent experiments with  $\geq 40$  metaphase spindles per condition.

Data information: Bars, 5  $\mu$ m. In (A), (C) and (D) red lines represent mean  $\pm$  SEM.

(poles, kinetochore fibers, and central spindle) (Zheng *et al*, 1991; Julian *et al*, 1993; Lajoie-Mazenc *et al*, 1994), we detected  $\gamma$ -tubulin along astral MTs (Fig 2A). The staining was punctate and was maintained from prophase to telophase. From anaphase onwards, when kinetochore fibers were depolymerized,  $\gamma$ -tubulin also appeared associated with interpolar MTs. Similar results were obtained using antibodies directed against Dgrip84, a component of the  $\gamma$ -TuSCs, or Dgp71WD, a non-grip component of the  $\gamma$ -TuRCs (Fig 2B). Depletion of Dgrip75 reduced  $\gamma$ -tubulin labelling along spindle and astral MTs, while a fraction of  $\gamma$ -tubulin staining was still retained at the centrosome (Fig 2C; Verollet *et al*, 2006). The detection of  $\gamma$ -tubulin along astral MTs throughout mitosis was confirmed by live-cell analysis of the  $\gamma$ -tubulin-GFP/mCherry- $\alpha$ -tubulin S2 cell line (supplementary Figs S1E, 2D and movie S2). This MT localization throughout the mitosis was also observed in the human HeLa cell line (Fig 2E). However, it is important to notice that it is more difficult to observe astral MTs in metaphase, as at this stage, MTs are shorter and much more labile compared to the other mitotic stages. Altogether, we conclude that  $\gamma$ -tubulin localizes along all mitotic MTs, most likely in the form of  $\gamma$ -TuRCs.

$\gamma$ -TuRCs have been shown to dock onto inner spindle MTs by the augmin complex (Goshima *et al*, 2008; Zhu *et al*, 2008; Lawo *et al*, 2009; Meireles *et al*, 2009; Uehara *et al*, 2009; Wainman *et al*, 2009; Kamasaki *et al*, 2013). For this reason, we tested whether augmin proteins also participate in the recruitment of  $\gamma$ -TuRCs on astral MTs. We addressed this question in HeLa cells because antibodies against *Drosophila* augmins showed poor specificity by IF. Two independent antibodies against the human augmin HAUS6 and one against HAUS2 decorated internal spindle MTs, and also astral MTs from prophase until late mitotic phases (supplementary Fig S3A–C). This localization was confirmed in live HeLa cells expressing HAUS2-GFP (supplementary movie S3). We also observed that HAUS6 and  $\gamma$ -tubulin partially co-localized along astral MTs throughout mitosis, as illustrated in metaphase and telophase (supplementary Fig S3C). siRNA treatment against HAUS6 resulted in pole fragmentation, which was not seen in depletions of  $\gamma$ -TuRC-specific proteins; and in additional defects that phenocopied the ones observed after depletion of  $\gamma$ -TuRC-specific components, such as metaphase arrest, low spindle MT density, increase of visible astral MTs and decrease of  $\gamma$ -tubulin staining on the spindle body and astral MTs (supplementary Fig S4Cd–f and

S4Dd–f; Lawo *et al*, 2009; Zhu *et al*, 2008). In these HAUS6-depletion conditions,  $\gamma$ -tubulin level was unchanged (supplementary Fig S4A). In contrast, HAUS6 labelling on spindle MTs persisted after depletion of GCP4 (supplementary Figs S4B, Cg–i and Dg–i). These results are consistent with the idea that the augmin complex participates in  $\gamma$ -TuRC recruitment along astral MTs as already described for recruitment along spindle MTs.

To support the idea that  $\gamma$ -TuRCs localizing along MTs contribute to proper spindle positioning, we chose to work in *Drosophila* cells where the cohesion of poles was still maintained after depletion of an augmin subunit. After Dgt6 RNAi treatment (condition in which the assembly of the  $\gamma$ -TuRCs and their recruitment to the poles were not affected), spindles rotated with higher angles compared to control spindles (supplementary Fig S4E–F). These results are similar to the ones described after Dgrip75 depletion (Fig 1A), supporting the idea that the  $\gamma$ -TuRCs associated to MTs are involved in spindle positioning.

 **$\gamma$ -TuRCs contribute to the regulation of astral MT dynamics**

The contribution of  $\gamma$ -TuRCs to spindle orientation and their presence on astral MTs led us to further characterize the function of these complexes during mitosis. Two main functions have been attributed to MT-associated  $\gamma$ -TuRCs, MT-dependent nucleation of secondary MTs and regulation of MT dynamics. Astral MTs usually appear unbranched, although during the prophase-prometaphase stages it has been reported that few clusters of peripheral MTs move to spindle poles to ensure proper spindle formation (Rusan *et al*, 2002; Tulu *et al*, 2003; Delaval *et al*, 2011). To test directly whether  $\gamma$ -TuRCs bound to the surface of astral MTs were involved in nucleation of secondary MTs, we compared the  $\alpha$ -tubulin fluorescence distal to the  $\gamma$ -tubulin spots (97%  $\pm$  12) with the measurements taken proximally, at a reference value of 100% (20 astral MTs, 5 cells, Inset Fig 2Ab). Since there was no significant variation in the intensity of tubulin staining proximally and distally of the  $\gamma$ -tubulin spots, we reasoned that in most of the cases no secondary, parallel MTs were emanating from these spots. Because an additional role of MT-bound  $\gamma$ -TuRCs has been described in stabilizing interphase MTs (Bouissou *et al*, 2009), we investigated whether depletion of a  $\gamma$ -TuRC component affected the dynamics of astral MTs during

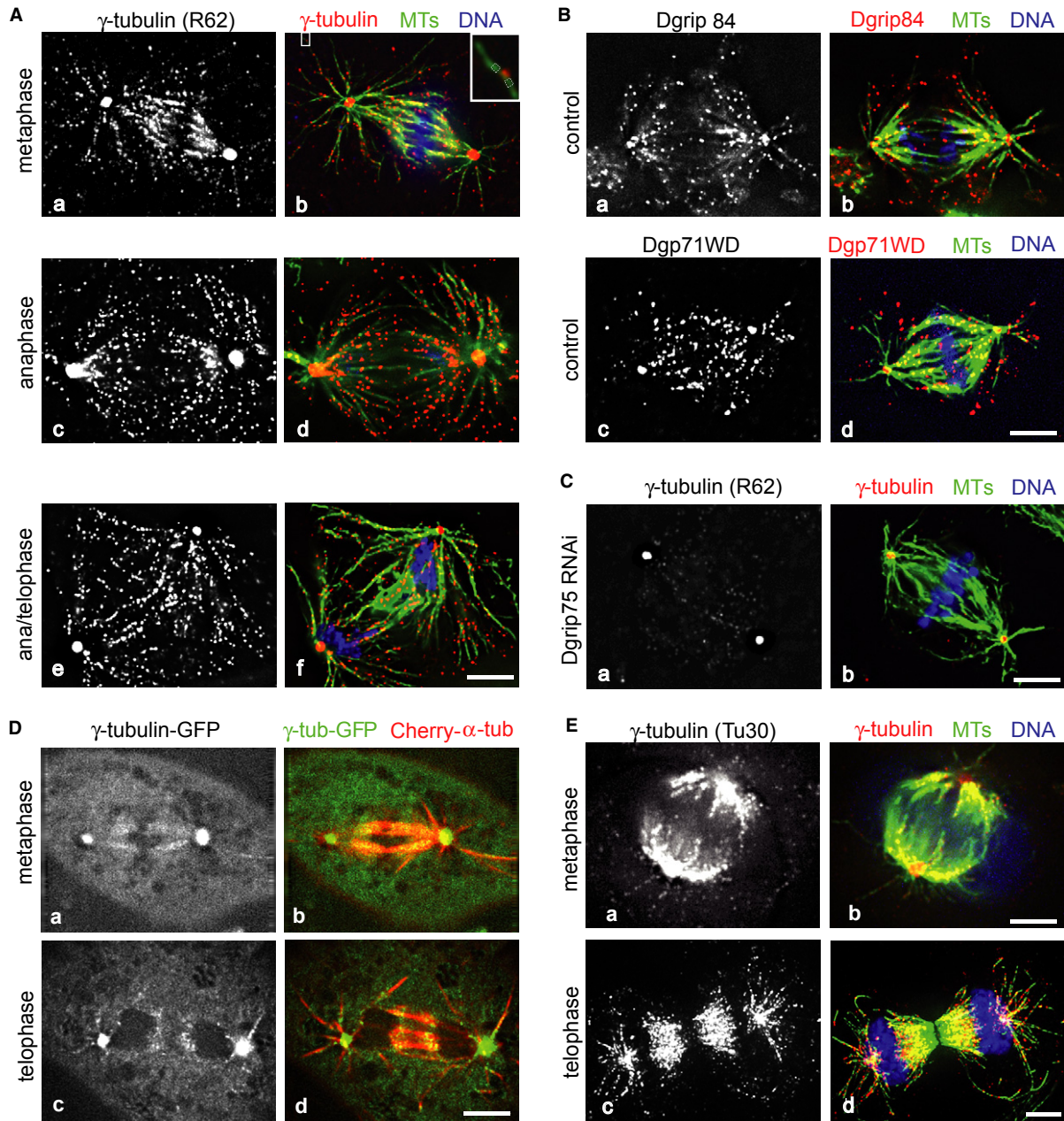


**Figure 2.**  $\gamma$ -TuRCs localize along astral MTs in *Drosophila* (A–D) and HeLa cells (E).

A–C Control (A–B) and Dgrip75-depleted (C) *Drosophila* S2R<sup>+</sup> cells were permeabilized and stained with antibodies against  $\gamma$ -tubulin (R62) (Aa, c, e and Ca) or Dgrip84 (Ba) or Dgp71WD (Bc). Merge (Ab, d, f; Bb,d; Cb): MTs are shown in green,  $\gamma$ -TuRC proteins in red and DNA in blue. Ab: Inset, 4-fold magnification,  $\alpha$ -tubulin immunofluorescence was measured in surfaces bounded by dotted lines distally and proximally to  $\gamma$ -tubulin spot.

D Live imaging of a  $\gamma$ -tubulin-GFP/mCherry- $\alpha$ -tubulin S2 cell in metaphase (a,b) and in telophase (c,d, see supplementary movie S2).

E HeLa cells were permeabilized and then stained with antibodies against  $\gamma$ -tubulin (Tu-30) (a,c). Merge (b,d): MTs are shown in green,  $\gamma$ -tubulin in red and DNA in blue.

Data information: Bars, 5  $\mu$ m.

metaphase (Fig 3A and supplementary movie S4). Down-regulation of Dgrip75 induced a significant increase in the dynamicity of astral MTs ( $8.2 \pm 0.2$   $\mu$ m/min versus  $6.3 \pm 0.1$   $\mu$ m/min in control cells, Fig 3B–C). The rates of MT growth and shrinkage were increased by roughly the same order of magnitude and the time spent in pause was decreased by about 30%. We also observed a slight but significant

increase in rescue frequency while the percentage of catastrophe transitions remained unchanged. This could explain a longer time spent at a growing state and consequently the increase of the astral MT length (supplementary Fig S1B, middle panel). We conclude that  $\gamma$ -TuRCs are involved in the regulation of astral MT dynamics, acting as a stabilizing factor.

### Spindle positioning defects in $\gamma$ -TuRC-depleted cells are rescued by suppressing MT dynamics

Disassembly of  $\gamma$ -TuRCs induced misorientation of mitotic spindles and increased astral MT dynamics. If the increase in MT dynamics is responsible for spindle positioning defects, we should be able to rescue these mitotic phenotypes by reducing MT dynamics. We therefore investigated, in HeLa cells, the effects of mild drug treatments that suppress MT dynamics on spindle orientations with or without GCP4 (Fig 4A) (Ganem & Compton, 2004). Addition of 5 nM taxol or 50 nM nocodazole reduced the extent of spindle misorientation induced after GCP4 siRNA. This indicates that the defects in spindle positioning consecutive to  $\gamma$ -TuRC loss-of-function are due to modification of MT dynamics.

To further confirm this notion, we altered MT dynamics by knocking-down a known protein regulator of MT dynamics. We focused on the plus-end-tracking proteins (+TIPs: EB1, Mast, Msp, Clip190), because some of these proteins have been shown to play a role in spindle positioning (for a review, see Lansbergen & Akhmanova, 2006). To select +TIPs that could antagonize the effects of  $\gamma$ -TuRC disassembly, we characterized the spindle morphology after the co-depletion of Dgrip75 with each individual +TIP in S2 cells. The highest percentages of rescued 'normal' bipolar spindles were obtained after simultaneous depletion of Dgrip75 with EB1 (supplementary Fig 5A–B). These results appeared particularly notable, since EB1 binds to MT plus-ends autonomously and is a key player in recruiting other +TIPs, and may thereby affect astral MT dynamics and spindle positioning (Rogers *et al*, 2002; Toyoshima & Nishida, 2007; Jiang & Akhmanova, 2011). In metaphase, the increases in spindle length, astral MT length and mitotic index observed after Dgrip75 depletion were rescued after down-regulation of EB1 (Fig 4B, supplementary Fig S5B–C). In a comparable manner, IF analysis showed that EB1 inhibition restored the main phenotypes induced by depletion of Dgrip128 (supplementary Fig S2B–C). Moreover, while individual down-regulation of Dgrip75 and EB1 resulted in spindle oscillations, spindles from cells depleted of both proteins no longer exhibited abnormal rotation (Fig 4C). Finally, in S2 cells with induced spindle polarity (Fig 1B), depleting both Dgrip75 and EB1 partially restored normal levels of spindle orientation, with a close range of orientation angles below 30°, compared to a more random distribution after individual depletion (Fig 4D). Since EB1 depletion resulted in shortening and almost complete loss of astral MTs (Fig 4Bc), it was not possible to measure their dynamic parameters. Nevertheless, MTs of cells co-depleted for both Dgrip75 and EB1 displayed dynamicity similar to controls ( $7.9 \pm 0.8 \mu\text{m}/\text{min}$  in co-depleted cells versus  $8.3 \pm 0.7 \mu\text{m}/\text{min}$  in control cells,  $n = 45$ ) and no significant modification in individual dynamic parameters (supplementary Fig S5D).

We performed a comparable study in HeLa cells. The individual depletion of EB1 induced defects in spindle length and orientation (Toyoshima & Nishida, 2007). The co-depletion of EB1 with GCP4, although less effective than single one, resulted in spindle orientation comparable to untreated cells (Fig 4E, supplementary Fig S5E). Altogether these results indicate that the  $\gamma$ -TuRCs act on spindle positioning through their role in MT dynamics.

### $\gamma$ -TuRC disassembly induces defective loading of EB1 and an increase of GTP-tubulin islands along MTs

The restoration of  $\gamma$ -TuRC-dependent mitotic defects by depletion of EB1 suggested a link between EB1 and  $\gamma$ -TuRCs. To explore this idea, we characterized the localization of EB1 after  $\gamma$ -TuRC disassembly. In *Drosophila* cells, there was a clear modification of EB1 staining after Dgrip75 depletion both in interphase and in mitosis (Fig 5A–C). While in control cells EB1 labelling was mainly restricted to the MT distal ends, in depleted cells the accumulation of EB1 to the tips was reduced but the length of EB1 staining along MTs was significantly increased. In mitosis, this phenotype was particularly visible at the level of astral MTs (for quantification see Fig 5B, right panel). These observations were confirmed in interphase using live analysis in an S2 cell line that stably expresses EB1-GFP (Fig 5D). Similar relocalizations of EB1 were obtained after depletion of GCP4 in interphase and mitotic HeLa cells (Fig 5E–F). Depletion of this  $\gamma$ -TuRC-specific component modified EB1 localization but did not change the total amount of EB1, as verified by Western blot analysis (supplementary Figs S2B, S5B and E). Thus, both in *Drosophila* and mammalian cells, the depletion of a  $\gamma$ -TuRC-specific protein disturbs EB1 loading to the MTs. Moreover in HeLa cells, depletion of the augmin-subunit HAUS6 also led to an increase of the length of EB1 staining along astral MTs (about 2.5-fold, supplementary Fig S6). These results support the idea that the association of  $\gamma$ -TuRCs to the MT surface is necessary for the proper localization of EB1.

Recent data show that EB1 has higher affinity to MT lattices formed from analogs of GTP-tubulin compared to lattices composed of GDP-tubulin. Thus, one hypothesis to explain the EB1 redistribution is a change in tubulin conformation after GCP4 depletion (Maurer *et al*, 2011, 2012; Seetapun *et al*, 2012). To explore this possibility, we took advantage of the antibody hMB11, directed against GTP-bound tubulin (Dimitrov *et al*, 2008). This antibody recognizes the growing MT tips and discrete spots randomly dispersed along MTs, referred to GTP-tubulin islands (Dimitrov *et al*, 2008; Nakata *et al*, 2011). In GCP4 siRNA-treated cells, the hMB11 patches on MTs appeared denser and brighter compared to control HeLa cells, suggesting a reduction of the distance between two adjacent GTP-tubulin islands (Figs 6A and B). We quantified the ratio of the surface covered by hMB11 IF to the surface of  $\alpha$ -tubulin IF, and detected an increase of about two-fold in GCP4-depleted cells compared to controls ( $0.45 \pm 0.02$  versus  $0.24 \pm 0.03$  in controls). Unfortunately, the constraints of the staining procedures used for hMB11 (only functional in permeabilized unfixed cells) did not allow a good conservation of the more unstable MTs, and therefore hindered the analysis of GTP-islands along astral MTs. The same technical limitations prevented the colocalization of tubulin-GTP and EB1, even using EB1-GFP or EB3-GFP HeLa cell lines. However, our study shows that  $\gamma$ -TuRC disassembly induces a redistribution of EB1 - concomitantly with an increase of GTP-tubulin along the MT lattice.

## Discussion

Using cultured cells and *Drosophila* neuroblasts, we demonstrate a novel role of  $\gamma$ -TuRCs in spindle positioning. We propose that spindle positioning is controlled by a balance created by antagonistic factors,

**Figure 3. Down-regulation of a  $\gamma$ -TuRC specific component enhances astral MT dynamics.**

- A Astral MTs were tracked for 120 s at 1 s intervals from cells selected in metaphase stages. Control GFP- $\alpha$ -tubulin S2 cell showing plus-ends of astral MTs (colored dots) (top panel). Magnification focusing on the behaviour of plus-end astral MTs at one pole over time (bottom panels). Some MTs disappear and others appear, see supplementary movie S4. Bars, 5  $\mu$ m.
- B The life history of astral MTs was analyzed to determine the dynamic parameters in control and Dgrip75-depleted cells,  $n > 150$  from 25 cells, 4 independent experiments.
- C Dynamicity of astral MTs in metaphase for control (white bars) and Dgrip75-depleted cells (black bars). The dynamicity that reflects the overall exchange of tubulin with the MT ends is calculated by dividing the sum of total length grown and shortened by the life span of the MT (Rusan *et al*, 2001). Data are shown as mean of 3 independent experiments with  $\geq 130$  astral MTs.

exerting stabilizing and destabilizing effects on astral MTs. We characterize  $\gamma$ -TuRCs and EB1 as representative examples for these two types of factors. Moreover, we show that EB1 redistribution is concomitant with an increase of GTP-tubulin islands along MTs. This suggests that  $\gamma$ -TuRC-dependent changes of MT dynamics involve switches of tubulin conformation that could affect EB1 localization.

We show that  $\gamma$ -TuRCs stabilize astral MTs. These results are consistent with our previous studies on  $\gamma$ -TuRCs associated to the lattice of interphase MTs that regulate dynamics by preventing MT depolymerization beyond the sites of  $\gamma$ -TuRC attachment (Bouissou *et al*, 2009). In comparison to interphase, the relative increase of MT dynamics upon  $\gamma$ -TuRC depletion is weaker during mitosis. Cell cycle differences, such as the composition of the cortical area or the balance of MT-associated proteins, may affect MT behaviour. Consistent with a role of  $\gamma$ -TuRCs in regulating astral MT dynamics, regular spindle orientation can be restored in the absence of  $\gamma$ -TuRCs at least partially, when cells are simultaneously treated with drugs that reduce MT dynamics, or when the level of plus-end-binding proteins that promote MT dynamics is lowered.

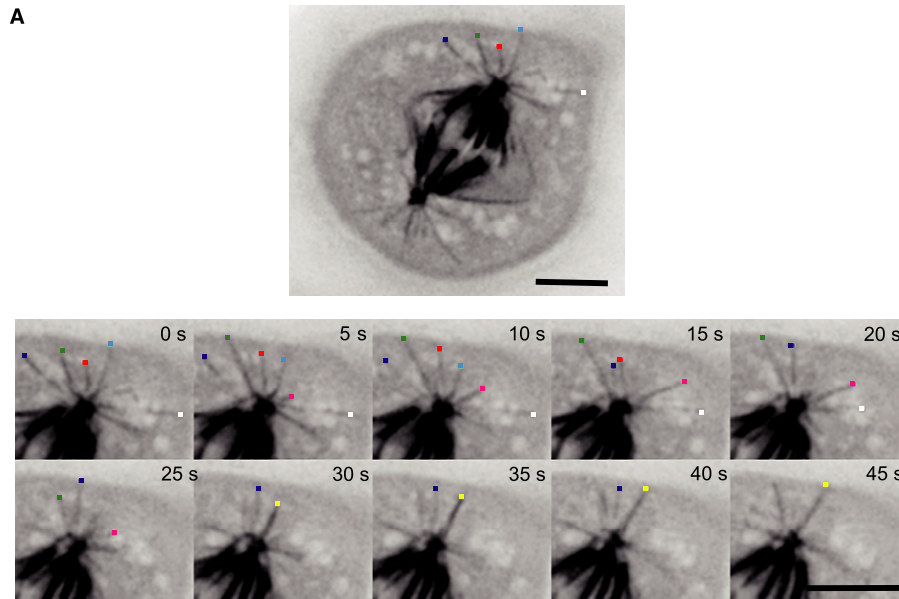
To investigate the mechanisms by which  $\gamma$ -TuRCs regulate the stability of astral MTs, we studied the localization of  $\gamma$ -TuRCs in mitotic cells. We observed astral localization of  $\gamma$ -TuRCs, evidenced by different IF procedures and confirmed by live-imaging. Such a localization pattern has not been described before, likely for three reasons. First, this localization may have been obscured by a large background of cytoplasmic  $\gamma$ -TuRCs (Moudjou *et al*, 1996; Raynaud-Messina *et al*, 2001). Second, only a small fraction of  $\gamma$ -tubulin is localized on MTs, and the faint, punctuate staining may have been overlooked previously. Third, astral MTs mostly appear as individual MTs, not organized in bundles like kinetochore fibers, and consequently associated proteins appear less concentrated. We also demonstrate that the recruitment of  $\gamma$ -TuRCs to astral MTs in mammalian cells is, at least partially, dependent on the augmin complexes, whereas augmin proteins are still present along MTs after  $\gamma$ -TuRC disassembly. These data suggest a recruitment of the augmin complexes on astral MTs prior to  $\gamma$ -tubulin complexes, or a pre-requisite of large complexes (including augmin and  $\gamma$ -TuRCs) forming in the cytoplasm before  $\gamma$ -TuRC recruitment. In addition to augmins, the protein Cdk5Rap2 may also be involved in binding  $\gamma$ -tubulin complexes to the MTs, since Cdk5Rap2 is known to interact with  $\gamma$ -TuRCs and concentrates partially at MT plus-ends, where it contributes to the regulation of MT dynamics (Fong *et al*, 2008, 2009; Choi *et al*, 2010).

So far, the main function that has been attributed to  $\gamma$ -TuRCs attached to the MT surface via augmin complexes is the nucleation of secondary MTs, to increase the density of kinetochore fibers (Luders & Stearns, 2007; Goshima *et al*, 2008; Zhu *et al*, 2008; Kamasaki *et al*, 2013). However, our study as well as previously published data on plant cells argue against a sole function of

MT-bound  $\gamma$ -TuRCs in secondary nucleation and suggest that these complexes have additional functions. First of all, our measurements of a homogeneous tubulin IF intensity along astral MTs indicate that no additional MTs have been nucleated at these specific sites. Moreover in plant cells, the majority of  $\gamma$ -TuRC foci associated to interphase MTs are not nucleating any other MTs, and the subset of  $\gamma$ -tubulin complexes active in generating new MTs appear enriched in the homolog of Mozart1 (Nakamura *et al*, 2010, 2012). Finally, a recently published study in *Arabidopsis* shows that the augmin subunit 8 binds to the MT plus-ends, regulates the dynamics of MT plus-ends and by this way controls MT reorientation in hypocotyls (Cao *et al*, 2013).

All these data lead us to propose a certain heterogeneity or plasticity in  $\gamma$ -TuRCs associated to the MT surface. In addition to their nucleation activity, some  $\gamma$ -TuRCs, by attaching to MTs, could exert a stabilizing effect on individual MTs, independent of their dormant potential to nucleate secondary MTs.  $\gamma$ -TuRCs along the MT surface may function in an analogous manner as a Microtubule Associated Protein (MAP), or if localized to the plus-end, increase stability similar to a cap. We suggest that the spindle orientation defects that we observe upon  $\gamma$ -TuRC-disassembly are not due to altered mechanisms of MT nucleation. First, we show that the activity of nucleation at the poles is comparable in control and  $\gamma$ -TuRC-deficient cells (supplementary Fig S1) and mitotic MTs in cells lacking the full  $\gamma$ -TuRC proteins possess a regular structure, with 13 protofilaments per diameter (Verollet *et al*, 2006). Moreover, suppression of MT dynamics is sufficient to restore spindle orientation (Fig 4). Besides, data in yeast suggest that mutations in individual components of the  $\gamma$ -tubulin complexes influence MT dynamics in a post-nucleation manner (Paluh *et al*, 2000; Fujita *et al*, 2002; Cuschieri *et al*, 2006; Masuda *et al*, 2006; Anders & Sawin, 2011). In addition, depletion of Dgp71WD or of an augmin subunit does not modify the quantity and the elongation of *de novo* nucleated MTs associated with acentriolar centers but does affect their stability (Moutinho-Pereira *et al*, 2009). This is consistent with previous data showing that in *Drosophila* cells the soluble pool of  $\alpha/\beta$  tubulin is not significantly changed after depletion of individual  $\gamma$ -TuRC grip-motif proteins (Rogers *et al*, 2008; Bouissou *et al*, 2009). Even if the soluble pool were slightly increased, the effects on MT dynamics would probably be minimal, since MT dynamics in cells, in contrast to the situation described *in vitro*, appear much more sensitive to the regulation by MT-associated proteins than to the concentration of free  $\alpha/\beta$  tubulin (Kinoshita *et al*, 2001; Goodwin & Vale, 2010).

Consistent with our hypothesis on altered MT dynamics, we observe a change in EB1 localization following depletion of  $\gamma$ -TuRC-specific subunits. EB1 is no longer concentrated at the MT plus-ends but rather distributed along MT side walls. Similar EB1 redistribution has been reported in other experimental setups affecting MT



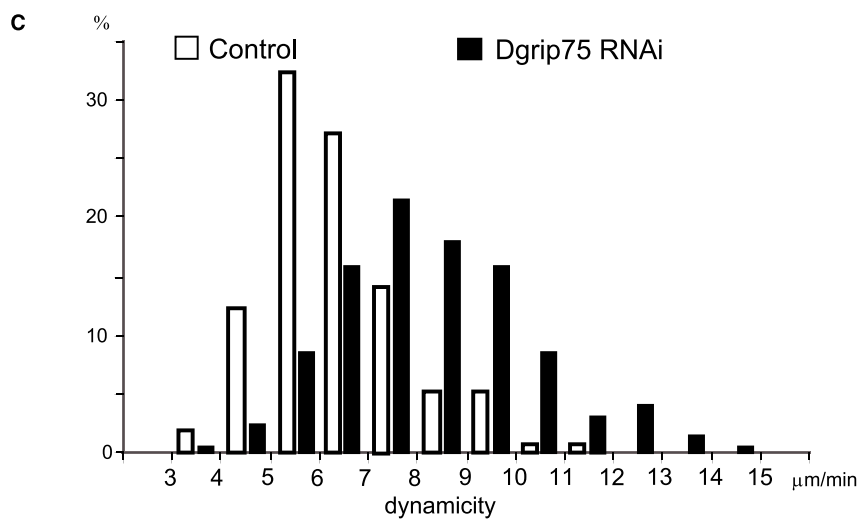
**B**

	Control	Dgrip75 RNA	Significance
growth rate (1)	7.4 ± 0.1	9.2 ± 0.2	***
shrinkage rate (1)	8.6 ± 0.2	10.4 ± 0.3	***
time in pause (2)	22 ± 0.7	16 ± 0.7	***
time in growth (2)	38 ± 1.3	47 ± 2.0	**
time in shrinkage (2)	40 ± 1.6	40 ± 1.8	n.s
catastrophe (3)	18.2 ± 0.6	18.8 ± 0.4	n.s
rescue (3)	15.1 ± 0.5	19.4 ± 0.6	*
<b>dynamicity (1)</b>	<b>6.3 ± 0.1</b>	<b>8.3 ± 0.2</b>	<b>**</b>

(1) Rate ( $\mu\text{m}/\text{min}$ )

(2) Time in a state (%)

(3) Transition frequencies (events/s X100)





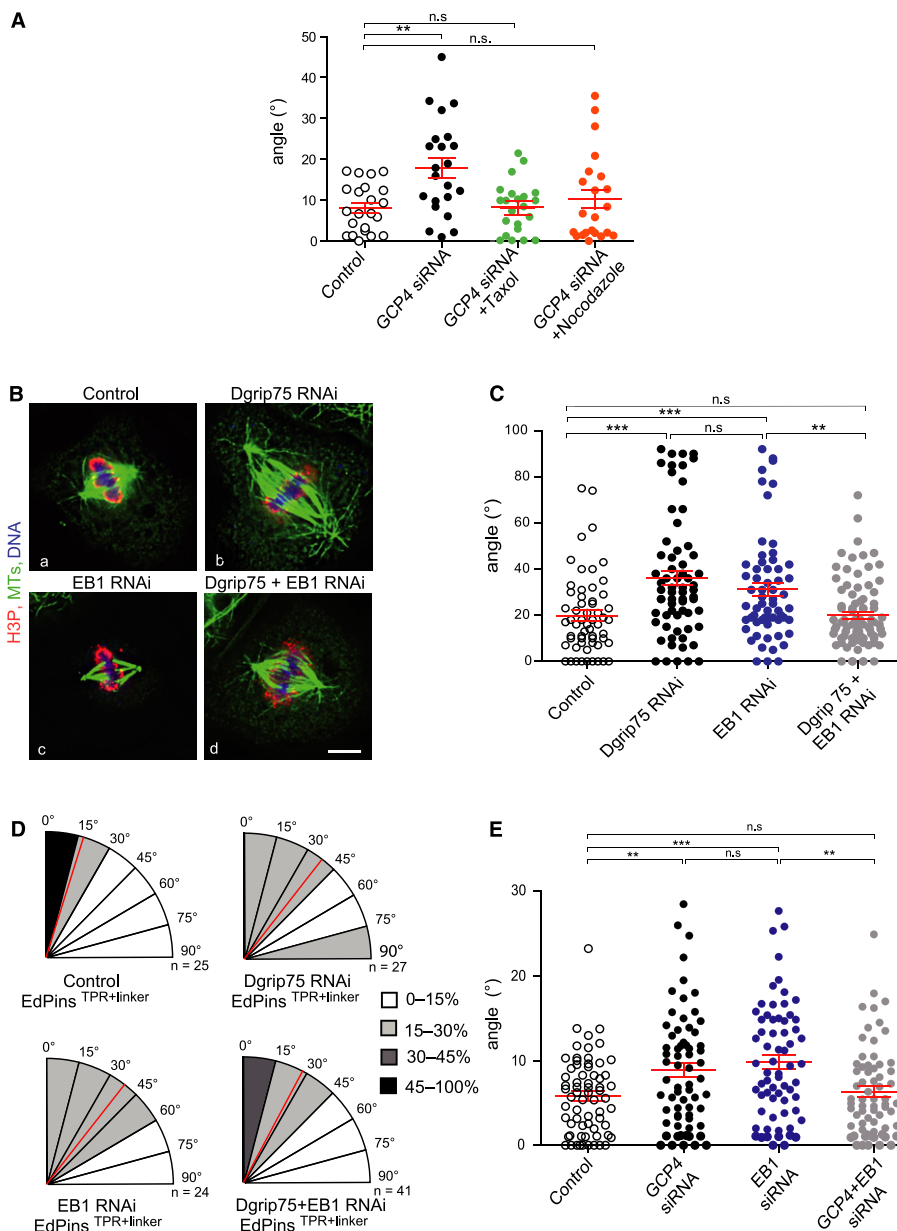


**Figure 4. Suppression of MT dynamics restores the defects in spindle positioning after  $\gamma$ -TuRC inhibition.**

- A Distribution of spindle angles in control and in GCP4-depleted HeLa cells, without or with MT drug treatment. HeLa cells were treated with 5 nM taxol or 50 nM nocodazole 5 h before immunostaining and angles were quantified as described in Fig 1C. These experiments have been performed twice with 22 analyzed bipolar spindles per condition.
- B Metaphase phenotypes obtained after co-depletion of Dgrip75 and EB1 in S2 cells. Control and RNAi-treated S2 cells were stained for  $\alpha$ -tubulin (green), H3P (red), and DNA (DAPI, blue). Bars, 5  $\mu$ m.
- C Quantification of spindle positioning after live microscopy in control cells (white circle), and in Dgrip75- (black circle), EB1- (blue circle) and Dgrip75+EB1-depleted cells (grey circle). Data are shown as mean of at least 3 independent experiments with  $\geq 55$  spindles.
- D Quantification of spindle orientation rescue in the S2 induced polarity model. Spindle angle repartition: the red line represents the median angle and n the number of measured spindles. Dgrip75 RNAi-Ed::mChery-Pins<sup>TRP+linker</sup> and EB1 RNAi-Ed::mChery-Pins<sup>TRP+linker</sup> conditions are not different but they significantly differ from the two others conditions ( $P < 0.001$ ). These data are representative of 2 independent experiments.
- E Distribution of spindle angles in control, GCP4-, EB1- and GCP4+EB1-depleted HeLa cells. This experiment has been performed twice with 66 analyzed spindles per condition.

Data information: In (A), (C) and (E) red lines represent mean  $\pm$  SEM.

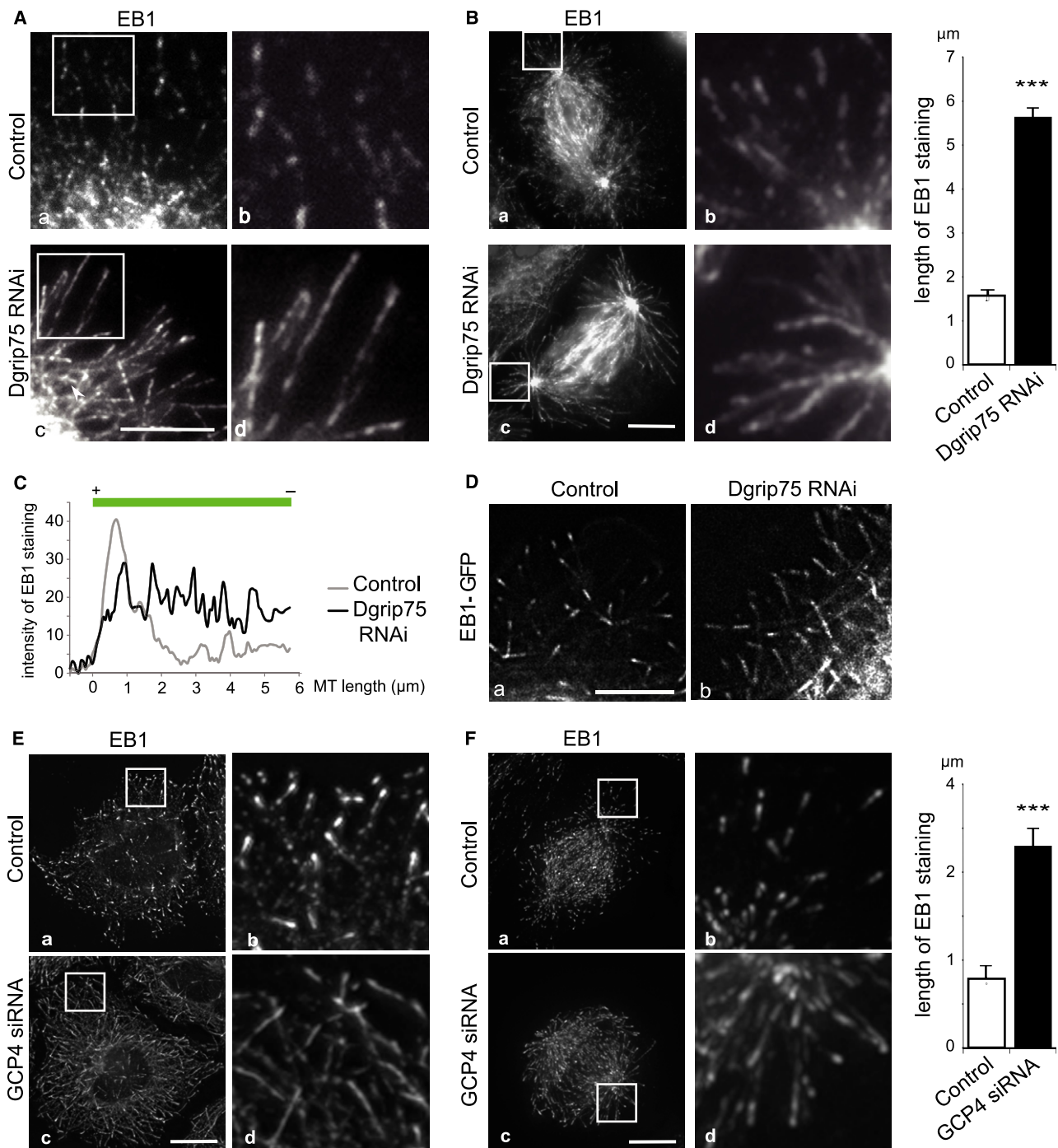


**Figure 5.**  $\gamma$ -TuRC depletion impairs EB1 loading in *Drosophila* (A–D) and in HeLa cells (E–F).

A–B Localization of EB1: control or Dgrip75-depleted S2 cells plated on ConA were stained with antibodies against EB1 in interphase (A) and in mitosis (B, left panel). Insets, 2.5-fold (A) or 5-fold (B) magnification. Right panel (B): quantification of length of EB1 staining along astral MTs in metaphase for control (white bars) and Dgrip75-depleted cells (black bars).

C Intensity of EB1 staining (arbitrary values) along interphase MT plus-ends. In control MTs (grey), an intense EB1 staining was concentrated over 1  $\mu$ m at the distal MT plus-end whereas in Dgrip75-depleted MTs (black), the staining was less intense at the tip and spread over 5  $\mu$ m. This graph was representative of 100 MTs from more than 10 cells analyzed per condition.

D Live imaging of interphase EB1-GFP S2 cells: control (a) or depleted of Dgrip75 (b).

E–F EB1 localization in control (a,b) or GCP4-depleted (c,d) HeLa cells in interphase (E) or in mitosis (F, left panel). (b,d) represent insets, 5-fold magnification. Right panel (F): Length of EB1 staining on astral MTs in metaphase for control (white bars) and GCP4-depleted cells (black bars).

Data information: Bars, 5  $\mu$ m.

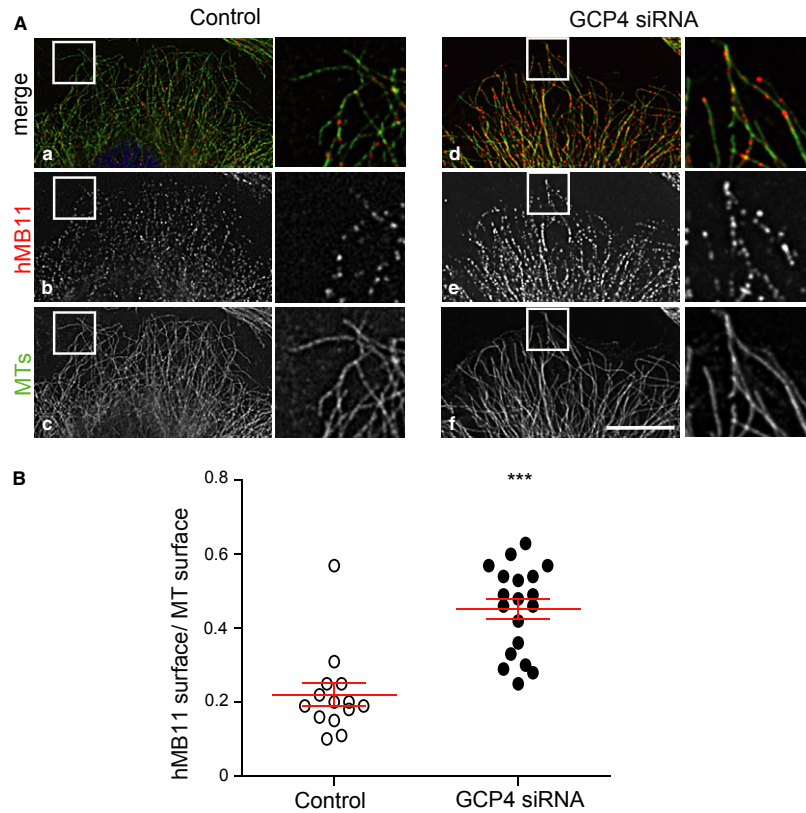


**Figure 6. Loss of  $\gamma$ -TuRCs increases GTP remnants on MTs in HeLa cells.**

- A** HeLa cell co-stained with a recombinant antibody, hMB11, that recognizes the GTP-bound conformation on tubulin (b,e: red), and antibody against  $\alpha$ -tubulin (c,f: green) and merge (a,d) in control and GCP4-depleted cells. Insets on the right of each image, 3-fold magnification. Bars, 5  $\mu$ m.
- B** Quantification of the ratio of hMB11 surface/MT surface, measured in the periphery of at least 12 separate cells. Each dot in the graph represents the value from one peripheral zone.

dynamics, for example following depletion of EB1 interactors, such as the XMAP215/Dis protein family or the p150<sup>Glued</sup> subunit of dyactin, or immunodepletion of  $\gamma$ -tubulin from frog egg extracts (Levy *et al*, 2006; Kawamura & Wasteney, 2008; Currie *et al*, 2011; Petry *et al*, 2013), and after treatment with MT-targeting agents (Pagano *et al*, 2012). However, a mechanistic explanation is lacking so far. One possibility would be that reduced affinity of EB1 to MT tips increases the pool of EB1 that might now bind to lower affinity sites on the MT lattice. Alternatively, and not mutually exclusive, changes in the size and intensity of EB1 staining after  $\gamma$ -TuRC depletion may result from alterations in GTP caps or GTP-remnants on MTs. We explored this possibility using the antibody hMB11, known to recognize a conformational state of tubulin, acquired upon binding of GTP (Dimitrov *et al*, 2008). EB1 and hMB11 antibodies have higher affinity for GTP-MTs compared to GDP-MTs *in vitro* (Dimitrov *et al*, 2008; Maurer *et al*, 2011, 2012; Seetapun *et al*, 2012) and both can colocalize as patches on the lattice of axonal MTs when EB1 is overexpressed (Nakata *et al*, 2011). So, the extended MT surface that was stained with both EB1 and hMB11 after  $\gamma$ -TuRC depletion may be due to altered tubulin conformation or a modified guanosine nucleotide status. This interpretation makes sense with a recent study that proposes that the effects between EB1 and the MT-associated protein XMAP215 on MT

dynamics don't rely on any direct interaction but rather on allosteric interaction through MT ends (Zanic *et al*, 2013). Abnormal loading of EB1 to the MTs after  $\gamma$ -TuRC disassembly may have itself a feedback on the balanced loading of +TIP complexes and also on the MT binding to the cell cortex. Therefore it may enhance any primary effects following the loss of  $\gamma$ -TuRCs, especially on spindle orientation. In any of the above discussed scenarios,  $\gamma$ -TuRCs may not interact directly with EB1. This is based on the observations (i) that EB1 is generally not enriched at sites of  $\gamma$ -TuRC localization, (ii) that a decrease of  $\gamma$ -TuRC along MTs leads to an increase of the length of EB1 staining, and (iii) that EB1 appears absent from sucrose gradient fractions corresponding to  $\gamma$ -TuRCs (B. Raynaud-Messina, unpublished data).

Oriented cell divisions appear critical for proper development and maintenance of tissue homeostasis. Moreover, emerging evidence reveals a link between spindle mis-orientation and a number of developmental diseases as well as tumorigenesis. The study of spindle positioning is therefore fundamental to both developmental biology and human pathologies (Lu & Johnston, 2013). We provide new mechanistic information for understanding this key event. Our results invoke  $\gamma$ -TuRCs as novel players in spindle orientation by indirectly controlling localization of EB1, a key protein involved in the physical interaction between mitotic spindle and cell cortex.

## Materials and Methods

### S2 and mammalian cell experiments

*Drosophila* Schneider S2 cells were stably transfected with a plasmid encoding GFP- $\alpha$ -tubulin or  $\gamma$ -tubulin-GFP/mCherry- $\alpha$ -tubulin (from G. Goshima, Nagoya University, Chikusa-ku, Nagoya, Japan) or EB1-GFP (from S. Carreno, Université de Montréal, Canada). RNA interference was performed according to (Verollet *et al*, 2006). The dsRNAs against Dgrip75, Dgrip128, Dgt6, EB1, Mast, Msp and Clip190 were generated from a library of *Drosophila* cDNA (ThermoFischer Scientific, Illkirch, France). *Drosophila* cells were treated with double-strand RNAs (dsRNA) at day 1 and harvested on day 5. The 'induced cell polarity' assay was carried out as previously described (Johnston *et al*, 2009). Briefly, 2 days after RNAi treatment, cells were transiently transfected with Ed fusion constructs using Effectene (QIAGEN, Courtaboeuf, France). At 48 h post-transfection, cells were induced with CuSO<sub>4</sub> (500 mM; Sigma-Aldrich, Saint-Quentin Fallavier, France) for 24 h to allow for Ed fusion protein expression. Cells were harvested, resuspended in fresh media, shaken (200 rpm) for 3 h to induce Ed-mediated cell-cell clusters and then plated for at least 4 h on glass coverslips before fixation.

HeLa cells expressing murine HAUS2::GFP from a BAC were provided by L. Pelletier (University of Toronto, Toronto, ON, Canada) (Lawo *et al*, 2009). EB1-GFP and EB3-GFP HeLa cell lines were established by A. Akhmanova (Utrecht University, The Netherlands). Cells were transfected with siRNA oligomers using lipofectamine RNAiMAX (ThermoFischer Scientific) according to the manufacturer. The following RNA oligonucleotides were used for silencing: GCP4: Silencer Select S25991 (ThermoFischer Scientific) for orientation experiments; HAUS6: previously reported oligonucleotide (ThermoFischer Scientific; Zhu *et al*, 2008); EB1: S225914 (ThermoFischer Scientific). For rescue experiments, we constructed stable Flp-In<sup>Tm</sup> T-Rex<sup>Tm</sup> HeLa cells (from S. Taylor, University of Manchester, UK) that express in an inducible manner a form of GCP4 resistant to siRNA treatment, following the protocol recommended by the manufacturer (ThermoFischer Scientific). Five hours after siRNA transfection, medium was replaced with fresh medium containing the inducer Doxycycline (1  $\mu$ g/ml; Clontech, Saint-Germain en Laye, France). Cells were analysed 72 h after siRNA transfection.

### Fly strains

*Drosophila w*<sup>118</sup> strains (as controls) and mutant strains *Dgrip75*<sup>175</sup> (Schnorrer *et al*, 2002) were used. For immunohistochemistry on brains, third instar larvae were dissected in PBS. The brains were collected and fixed in PBS containing 4% paraformaldehyde, 0.1% Triton X-100 for 20 min at room temperature and processed as described (Betschinger *et al*, 2006) modified as (Goodwin & Vale, 2010). Brains were incubated overnight with mAb anti-Miranda (1:20; a kind gift of F. Matsuzaki), anti-centrosomin (1:500; a kind gift of T. Kaufman) and anti-phospho-histone H3 (1:2000; Upstate Biotechnology). The pictures were captured with a Leica SP5 laser scanning confocal microscope equipped with a 63 $\times$  oil immersion objective and analyzed using ImageJ.

### Antibodies and drugs

Mouse monoclonal antibodies T-5168 (Sigma-Aldrich) and 1501 (Millipore, Saint-Quentin en Yvelines, France) were used to stain  $\alpha$ -tubulin and actin, respectively. The following rabbit antibodies were used: R62 against *Drosophila* 23C  $\gamma$ -tubulin (Raynaud-Messina *et al*, 2004), R367 against Dgrip84, R300 against Dgrip75, and R267 against Dgp71WD (Verollet *et al*, 2006). We also used rabbit antibodies against Dgrip128 (from Y. Zheng, Howard Hughes Institute, Baltimore, MD, USA), EB1 (from S. Rogers, University of North Carolina, USA), phospho-histone3 (PH3) (1:500) (Upstate, Millipore), and GFP (Abcam, Cambridge, UK), Dgt6 (from P. Somma, Università di Roma, Roma, Italia). In HeLa cells or extracts, we used mouse anti- $\gamma$ -tubulin TU-30 (1:500) (Exbio, Vestec, Czech Republic) or rabbit anti- $\gamma$ -tubulin R75 (1:1000) (Lajoie-Mazenc *et al*, 1994), rabbit anti- $\alpha$ -tubulin (1:100) (Abcam) or mouse anti- $\alpha$ -tubulin T-5168 (1:1000) (Sigma-Aldrich), rabbit anti-HAUS6 (1:500) (from J. Lüders, Institute for Research in Biomedicine, Barcelona, Spain), anti-HAUS6 (1:500), anti-HAUS2 (1:200) (from L. Pelletier, University of Toronto, Toronto, ON, Canada), anti-GCP4 (Fava *et al*, 1999), anti-EB1 (BD Transduction, Le pont de Claix, France) and human hMB11 against GTP-MTs (1:400) (from F. Perez, Institut Curie, France). For MT drug treatments, cells were treated with 50 nM Nocodazole (Sigma-Aldrich) or 5 nM Taxol (Sigma-Aldrich) 5 h before fixation.

### Western blotting and cytological analysis

Protein extracts from S2 cells (Raynaud-Messina *et al*, 2004; Colombie *et al*, 2006) were prepared and subjected to Western blot analyses (7.5% polyacrylamide gel and SDS). HeLa cells were lysed, sonicated and 40  $\mu$ g of total protein extracts were subjected to Western blotting. S2 GFP- $\alpha$ -tubulin cells, cultured on 0.5 mg/ml ConA-coated coverslips for at least 3 h, were fixed with pre-cooled -20°C methanol for 10 min and then immunostained (Verollet *et al*, 2006). To detect  $\gamma$ -tubulin, Dgrip84 and Dgp71WD along MTs, S2R<sup>+</sup> cells (Yanagawa *et al*, 1998) were permeabilized, fixed and stained as described (Bouissou *et al*, 2009). HeLa cells were permeabilized for 2 min in PEM (100 mM Pipes, 1 mM EGTA, 2 mM MgCl<sub>2</sub>, pH 6.8) containing 0.02% v/v Saponine, and washed with PEM containing 4% polyethylene glycol. Then, cells were fixed for 10 min in 3.7% paraformaldehyde in PEM, containing 1% dimethyl sulfoxide, and for 15 min in 3.7% paraformaldehyde in 50 mM sodium carbonate buffer, pH 10, for  $\gamma$ -tubulin staining. Alternatively, for staining of HAUS proteins, cells were fixed in cold methanol after permeabilization. For most stainings in HeLa cells, we performed standard protocols (Lajoie-Mazenc *et al*, 1994). The labelling with hMB11 was done according to the procedure described by (Dimitrov *et al*, 2008). For the regrowth assays, S2 cells were fixed at various times after 2 h of cold exposure and then stained for  $\alpha$ -tubulin.

Fluorescence microscopy was performed with Deltavision RT equipment on an Olympus IX71 microscope, using a 100 $\times$  1.4 NA- or a 60 $\times$  1.42 NA-objective. Images were obtained with a CoolSnap camera, subsequently de-convolved (ratio conservative method), and optical sections were projected. The lengths of astral MTs and spindles, the spindle orientation, the intensity, the length of EB1 staining, the MT fluorescence intensity and the ratio hMB11signal/MT surface were measured using ImageJ. All images were prepared for publication using Photoshop software (Adobe, Dell, Saint-Ouen, France).

## Live imaging of MTs

*Drosophila* S2 GFP- $\alpha$ -tubulin and  $\gamma$ -tubulin-GFP/mCherry- $\alpha$ -tubulin cells were grown on ConA-coated coverslips. For MT dynamics parameters, images were acquired at 1 s-intervals for 120 s with Deltavision RT equipment (24°C) and deconvolved as in immunofluorescence analysis. Astral MT plus-ends were tracked using manual tracking plugin of ImageJ software. Dynamic parameters were defined and calculated as in (Bouissou et al, 2009). For the determination of spindle rotation, S2 GFP- $\alpha$ -tubulin cells ( $7.10^4$  cells/ml) were plated directly on 96-well glass-bottom plates (Greiner) at 25°C and imaged with a wide-field microscope (DMIRBE; Leica, Nanterre, France) and a MicroMax cooled CCD camera controlled by MetaMorph 6.1 software (MDS Analytical Technologies, Sunnyvale, CA, USA). Images were acquired at 5 min-intervals for 12 h with Z series of ten 1  $\mu$ m sections. We generated maximum intensity projections with MetaMorph and measured the maximum angle between anaphase axis and the spindle during prometaphase/metaphase stages, using ImageJ. For imaging HeLa expressing HAUS2::GFP, we added 1  $\mu$ M of Hoechst 33342 to the media, containing 20 mM of HEPES.

## Statistical analysis

Data sets representative of at least three independent experiments were analyzed for statistics using a Chi-square test (for % of time in pause, % of prophase with short MT asters and % of spindles with rotation angle  $>20^\circ$ ), or an unpaired Student *t*-test and One-way ANOVA (for all other data), with confidence intervals of 99%. Statistical analysis was performed using GraphPad Prism version 5 (GraphPad software, Inc., La Jolla, CA, USA). For MT dynamic parameters, values are given as mean  $\pm$  s.e.m. \*\*\* means highly statistically significant ( $P < 0.0001$ ), \*\* statistically significant ( $P < 0.001$ ) and n.s. not significant.

**Supplementary information** for this article is available online: <http://emboj.embopress.org>

## Acknowledgements

We thank Drs. A. Akhmanova, G. Goshima, T. Kaufman, J. Lüders, F. Matsuzaki, L. Pelletier, S. Rogers, P. Somma, S. Taylor, and Y. Zheng for the donation of cell lines and antibodies. We thank S. Carreno, C. Roubinet, H. Foussard, and the Plate-Forme IBISA, Toulouse for assistance in microscopy. We thank HM Boubon for the maintenance of fly strains and M. Wright for helpful discussions. This work was funded by grants from the Association pour la Recherche sur le Cancer (4720XP0230F and 1094), Centre National de la Recherche Scientifique, and Pierre Fabre Laboratories, and support for equipment was provided by the Fonds Européens de Développement Economique Régional.

## Author contributions

AB, CV, HF, LH, YB, FP, AM, BRM – To conception, design and analysis of the data; AB, CV, AM, BRM – Experiments. AB, CV, AM, BRM – Writing.

## Conflict of interest

The authors declare that they have no conflict of interest.

## References

- Anders A, Lourenco PC, Sawin KE (2006) Noncore components of the fission yeast gamma-tubulin complex. *Mol Biol Cell* 17: 5075–5093
- Anders A, Sawin KE (2011) Microtubule stabilization in vivo by nucleation- incompetent gamma-tubulin complex. *J Cell Sci* 124: 1207–1213
- Bahtz R, Seidler J, Arnold M, Haselmann-Weiss U, Antony C, Lehmann WD, Hoffmann I (2012) GCP6 is a substrate of Plk4 and required for centriole duplication. *J Cell Sci* 125: 486–496
- Barbosa V, Yamamoto RR, Henderson DS, Glover D (2000) Mutation of a *Drosophila* gamma tubulin ring complex subunit encoded by *discs degenerate-4* differentially disrupts centrosomal protein localization. *Genes Dev* 14: 3126–3139
- Betschinger J, Mechtler K, Knoblich JA (2006) Asymmetric segregation of the tumor suppressor brat regulates self-renewal in *Drosophila* neural stem cells. *Cell* 124: 1241–1253
- Bouissou A, Verollet C, Sousa A, Sampaio P, Wright M, Sunkel CE, Merdes A, Raynaud-Messina B (2009) {gamma}-Tubulin ring complexes regulate microtubule plus end dynamics. *J Cell Biol* 187: 327–334
- Cao L, Wang L, Zheng M, Cao H, Ding L, Zhang X, Fu Y (2013) Arabidopsis AUGMIN subunit8 is a microtubule plus-end binding protein that promotes microtubule reorientation in hypocotyls. *Plant Cell* 25: 2187–2201
- Choi YK, Liu P, Sze SK, Dai C, Qi RZ (2010) CDK5RAP2 stimulates microtubule nucleation by the gamma-tubulin ring complex. *J Cell Biol* 191: 1089–1095
- Colombie N, Verollet C, Sampaio P, Moisan A, Sunkel C, Bourbon HM, Wright M, Raynaud-Messina B (2006) The *Drosophila* gamma-tubulin small complex subunit Dgrip84 is required for structural and functional integrity of the spindle apparatus. *Mol Biol Cell* 17: 272–282
- Currie JD, Stewman S, Schimizzi G, Slep KC, Ma A, Rogers SL (2011) The microtubule lattice and plus-end association of *Drosophila* Mini spindles is spatially regulated to fine-tune microtubule dynamics. *Mol Biol Cell* 22: 4343–4361
- Cuschieri L, Miller R, Vogel J (2006) Gamma-tubulin is required for proper recruitment and assembly of Kar9-Bim1 complexes in budding yeast. *Mol Biol Cell* 17: 4420–4434
- Delaval B, Bright A, Lawson ND, Doxsey S (2011) The cilia protein IFT88 is required for spindle orientation in mitosis. *Nat Cell Biol* 13: 461–468
- Dimitrov A, Quesnoit M, Moutel S, Cantaloube I, Pous C, Perez F (2008) Detection of GTP-tubulin conformation in vivo reveals a role for GTP remnants in microtubule rescues. *Science* 322: 1353–1356
- Fava F, Raynaud Messina B, Leung Tack J, Mazzolini L, Li M, Guillemot JC, Cachot D, Tollon Y, Ferrara P, Wright M (1999) Human 76p: a new member of the gamma-tubulin-associated protein family. *J Cell Biol* 147: 857–868
- Fong KW, Choi YK, Rattner JB, Qi RZ (2008) CDK5RAP2 is a pericentriolar protein that functions in centrosomal attachment of the gamma-tubulin ring complex. *Mol Biol Cell* 19: 115–125
- Fong KW, Hau SY, Kho YS, Jia Y, He L, Qi RZ (2009) Interaction of CDK5RAP2 with EB1 to track growing microtubule tips and to regulate microtubule dynamics. *Mol Biol Cell* 20: 3660–3670
- Fujita A, Vardy L, Garcia MA, Toda T (2002) A fourth component of the fission yeast  $\gamma$ -tubulin complex, Alp16, is required for cytoplasmic microtubule integrity and becomes indispensable when  $\gamma$ -tubulin function is compromised. *Mol Biol Cell* 13: 2360–2373

- Ganem NJ, Compton DA (2004) The KinI kinesin Kif2a is required for bipolar spindle assembly through a functional relationship with MCAK. *J Cell Biol* 166: 473–478
- Goodwin SS, Vale RD (2010) Patronin regulates the microtubule network by protecting microtubule minus ends. *Cell* 143: 263–274
- Goshima G, Mayer M, Zhang N, Stuurman N, Vale RD (2008) Augmin: a protein complex required for centrosome-independent microtubule generation within the spindle. *J Cell Biol* 181: 421–429
- Haren L, Remy M-H, Bazin I, Callebaut I, Wright M, Merdes A (2006) NEDD1-dependent recruitment of the  $\gamma$ -tubulin ring complex to the centrosome is necessary for centriole duplication and spindle assembly. *J Cell Biol* 172: 505–515
- Horio T, Uzawa S, Jung MK, Oakley BR, Tanaka K, Yanagida M (1991) The fission yeast gamma-tubulin is essential for mitosis and is localized at microtubule organizing centers. *J Cell Sci* 99: 693–700
- Hutchins JR, Toyoda Y, Hegemann B, Poser I, Heriche JK, Sykora MM, Augsburg M, Hudecz O, Buschhorn BA, Bulkescher J, Conrad C, Comartin D, Schleiffer A, Sarov M, Pozniakovskiy A, Slabicki MM, Schloissnig S, Steinmacher I, Leuschner M, Szykora A et al (2010) Systematic analysis of human protein complexes identifies chromosome segregation proteins. *Science* 328: 593–599
- Izumi N, Fumoto K, Izumi S, Kikuchi A (2008) GSK-3 $\beta$  regulates proper mitotic spindle formation in cooperation with a component of the gamma-tubulin ring complex, GCP5. *J Biol Chem* 283: 12981–12991
- Jiang K, Akhmanova A (2011) Microtubule tip-interacting proteins: a view from both ends. *Curr Opin Cell Biol* 23: 94–101
- Johnston CA, Hirono K, Prehoda KE, Doe CQ (2009) Identification of an Aurora-A/Pins/LINKER/Dlg spindle orientation pathway using induced cell polarity in S2 cells. *Cell* 138: 1150–1163
- Julian M, Tollon Y, Lajoie-Mazenc I, Moisan A, Mazarguil H, Puget A, Wright M (1993) Gamma-tubulin participates in the formation of the midbody during cytokinesis in mammalian cells. *J Cell Sci* 105: 145–156
- Kamasaki T, O'Toole E, Kita S, Osumi M, Usukura J, McIntosh JR, Goshima G (2013) Augmin-dependent microtubule nucleation at microtubule walls in the spindle. *J Cell Biol* 202: 25–33
- Kawamura E, Wasteneys GO (2008) MOR1, the Arabidopsis thaliana homologue of Xenopus MAP215, promotes rapid growth and shrinkage, and suppresses the pausing of microtubules in vivo. *J Cell Sci* 121: 4114–4123
- Kinoshita K, Arnal I, Desai A, Drechsel DN, Hyman AA (2001) Reconstitution of physiological microtubule dynamics using purified components. *Science* 294: 1340–1343
- Knop M, Schiebel E (1997) Spc98p and Spc97p of the yeast gamma-tubulin complex mediate binding to the spindle pole body via their interaction with Spc110p. *EMBO J* 16: 6985–6995
- Kollman JM, Merdes A, Mourey L, Agard DA (2011) Microtubule nucleation by gamma-tubulin complexes. *Nat Rev Mol Cell Biol* 12: 709–721
- Kunda P, Baum B (2009) The actin cytoskeleton in spindle assembly and positioning. *Trends Cell Biol* 19: 174–179
- Lajoie-Mazenc I, Tollon Y, Détraves C, Julian M, Moisan A, Gueth-Hallonet C, Debec A, Salles-Passador I, Puget A, Mazarguil H, Raynaud-Messina B, Wright M (1994) Recruitment of antigenic gamma-tubulin during mitosis in animal cells: presence of gamma-tubulin in the mitotic spindle. *J Cell Sci* 107: 2825–2837
- Lansbergen G, Akhmanova A (2006) Microtubule plus end: a hub of cellular activities. *Traffic* 7: 499–507
- Lawo S, Bashkurov M, Mullin M, Ferreria MG, Kittler R, Habermann B, Tagliaferro A, Poser I, Hutchins JR, Hegemann B, Pinchev D, Buchholz F, Peters JM, Hyman AA, Gingras AC, Pelletier L (2009) HAUS, the 8-subunit human Augmin complex, regulates centrosome and spindle integrity. *Curr Biol* 19: 816–826
- Levy JR, Sumner CJ, Caviston JP, Tokito MK, Ranganathan S, Ligon LA, Wallace KE, LaMonte BH, Harmison GG, Puls I, Fischbeck KH, Holzbaur EL (2006) A motor neuron disease-associated mutation in p150Glued perturbs dynactin function and induces protein aggregation. *J Cell Biol* 172: 733–745
- Lu MS, Johnston CA (2013) Molecular pathways regulating mitotic spindle orientation in animal cells. *Development* 140: 1843–1856
- Luders J, Patel UK, Stearns T (2006) GCP-WD is a gamma-tubulin targeting factor required for centrosomal and chromatin-mediated microtubule nucleation. *Nat Cell Biol* 8: 137–147
- Luders J, Stearns T (2007) Microtubule-organizing centres: a re-evaluation. *Nat Rev Mol Cell Biol* 8: 161–167
- Masuda H, Miyamoto R, Haraguchi T, Hiraoka Y (2006) The carboxy-terminus of Alp4 alters microtubule dynamics to induce oscillatory nuclear movement led by the spindle pole body in *Schizosaccharomyces pombe*. *Genes Cells* 11: 337–352
- Maurer SP, Bieling P, Cope J, Hoenger A, Surrey T (2011) GTPgammaS microtubules mimic the growing microtubule end structure recognized by end-binding proteins (EBs). *Proc Natl Acad Sci U S A* 108: 3988–3993
- Maurer SP, Fourniol FJ, Bohner G, Moores CA, Surrey T (2012) EBs recognize a nucleotide-dependent structural cap at growing microtubule ends. *Cell* 149: 371–382
- Meireles AM, Fisher KH, Colombie N, Wakefield JG, Ohkura H (2009) Wac: a new Augmin subunit required for chromosome alignment but not for acentrosomal microtubule assembly in female meiosis. *J Cell Biol* 184: 777–784
- Moritz M, Braunfeld MB, Sedat JW, Alberts B, Agard DA (1995) Microtubule nucleation by  $\gamma$ -tubulin-containing rings in the centrosome. *Nature* 378: 638–640
- Moudjou M, Bordes N, Paintrand M, Bornens M (1996) Gamma-tubulin in mammalian cells: the centrosomal and the cytosolic forms. *J Cell Sci* 109: 875–887
- Moutinho-Pereira S, Debec A, Maiato H (2009) Microtubule cytoskeleton remodeling by acentriolar microtubule-organizing centers at the entry and exit from mitosis in *Drosophila* somatic cells. *Mol Biol Cell* 20: 2796–2808
- Nakamura M, Ehrhardt DW, Hashimoto T (2010) Microtubule and katanin-dependent dynamics of microtubule nucleation complexes in the acentrosomal Arabidopsis cortical array. *Nat Cell Biol* 12: 1064–1070
- Nakamura M, Yagi N, Kato T, Fujita S, Kawashima N, Ehrhardt DW, Hashimoto T (2012) Arabidopsis GCP3-interacting protein 1/MOZART 1 is an integral component of the gamma-tubulin-containing microtubule nucleating complex. *Plant J* 71: 216–225
- Nakata T, Niwa S, Okada Y, Perez F, Hirokawa N (2011) Preferential binding of a kinesin-1 motor to GTP-tubulin-rich microtubules underlies polarized vesicle transport. *J Cell Biol* 194: 245–255
- Oakley BR, Oakley CE, Yoon Y, Jung MK (1990) Gamma-tubulin is a component of the spindle pole body that is essential for microtubule function in *Aspergillus nidulans*. *Cell* 61: 1289–1301
- Oegema K, Wiese C, Martin OC, Milligan RA, Iwamatsu E, Mitchison TJ, Zheng Y (1999) Characterization of two related *Drosophila*  $\gamma$ -tubulin complexes that differ in their ability to nucleate microtubules. *J Cell Biol* 144: 721–733

- Pagano A, Honore S, Mohan R, Berges R, Akhmanova A, Braguer D (2012) Epthilone B inhibits migration of glioblastoma cells by inducing microtubule catastrophes and affecting EB1 accumulation at microtubule plus ends. *Biochem Pharmacol* 84: 432–443
- Paluh JL, Nogales E, Oakley BR, McDonald K, Pidoux AL, Cande WZ (2000) A mutation in gamma-tubulin alters microtubule dynamics and organization and is synthetically lethal with the kinesin-like protein pkl1p. *Mol Biol Cell* 11: 1225–1239
- Pearson CG, Bloom K (2004) Dynamic microtubules lead the way for spindle positioning. *Nat Rev Mol Cell Biol* 5: 481–492
- Petry S, Groen AC, Ishihara K, Mitchison TJ, Vale RD (2013) Branching microtubule nucleation in *Xenopus* egg extracts mediated by augmin and TPX2. *Cell* 152: 768–777
- Raynaud-Messina B, Debec A, Tollon Y, Garès M, Wright M (2001) Differential properties of the two *Drosophila*  $\gamma$ -tubulin isoatypes. *Eur J Cell Biol* 80: 643–649
- Raynaud-Messina B, Mazzolini L, Moisan A, Cirinesi AM, Wright M (2004) Elongation of centriolar microtubule triplets contributes to the formation of the mitotic spindle in gamma-tubulin-depleted cells. *J Cell Sci* 117: 5497–5507
- Raynaud-Messina B, Merdes A (2007) gamma-tubulin complexes and microtubule organization. *Curr Opin Cell Biol* 19: 24–30
- Rogers GC, Rusan NM, Peifer M, Rogers SL (2008) A multicomponent assembly pathway contributes to the formation of acentrosomal microtubule arrays in interphase *Drosophila* cells. *Mol Biol Cell* 19: 3163–3178
- Rogers SL, Rogers GC, Sharp DJ, Vale RD (2002) *Drosophila* EB1 is important for proper assembly, dynamics, and positioning of the mitotic spindle. *J Cell Biol* 158: 873–884
- Rusan NM, Fagerstrom CJ, Yvon AM, Wadsworth P (2001) Cell cycle-dependent changes in microtubule dynamics in living cells expressing green fluorescent protein-alpha tubulin. *Mol Biol Cell* 12: 971–980
- Rusan NM, Tulu US, Fagerstrom C, Wadsworth P (2002) Reorganization of the microtubule array in prophase/prometaphase requires cytoplasmic dynein-dependent microtubule transport. *J Cell Biol* 158: 997–1003
- Schnorrer F, Luschnig S, Koch I, Nüsslein-Volhard C (2002)  $\gamma$ -tubulin 37C and  $\gamma$ -tubulin ring complex protein 75 are essential for bicoid RNA localization during *Drosophila* oogenesis. *Dev Cell* 3: 685–695
- Seetapun D, Castle BT, McIntyre AJ, Tran PT, Odde DJ (2012) Estimating the microtubule GTP cap size in vivo. *Curr Biol* 22: 1681–1687
- Siller KH, Doe CQ (2009) Spindle orientation during asymmetric cell division. *Nat Cell Biol* 11: 365–374
- Sunkel CE, Gomes R, Sampaio P, Perdigo J, Gonzalez C (1995) Gamma-tubulin is required for the structure and function of the microtubule organizing centre in *Drosophila* neuroblasts. *EMBO J* 14: 28–36
- Teixido-Travesa N, Roig J, Luders J (2012) The where, when and how of microtubule nucleation - one ring to rule them all. *J Cell Sci* 125: 4445–4456
- Teixido-Travesa N, Villen J, Lacasa C, Bertran MT, Archinti M, Gygi SP, Caelles C, Roig J, Luders J (2010) The  $\gamma$ TuRC revisited: a comparative analysis of interphase and mitotic human  $\gamma$ TuRC re-defines the set of core components and identifies the novel subunit GCP8. *Mol Biol Cell* 22: 3963–3972
- Toyoshima F, Nishida E (2007) Integrin-mediated adhesion orients the spindle parallel to the substratum in an EB1- and myosin X-dependent manner. *EMBO J* 26: 1487–1498
- Tulu US, Rusan NM, Wadsworth P (2003) Peripheral, non-centrosome-associated microtubules contribute to spindle formation in centrosome-containing cells. *Curr Biol* 13: 1894–1899
- Uehara R, Nozawa RS, Tomioka A, Petry S, Vale RD, Obuse C, Goshima G (2009) The augmin complex plays a critical role in spindle microtubule generation for mitotic progression and cytokinesis in human cells. *Proc Natl Acad Sci U S A* 106: 6998–7003
- Vardy L, Toda T (2000) The fission yeast  $\gamma$ -tubulin complex is required in G1 phase and is a component of the spindle assembly checkpoint. *EMBO J* 19: 6098–6111
- Venkatram S, Tasto JJ, Feoktistova A, Jennings JL, Link AJ, Gould KL (2004) Identification and characterization of two novel proteins affecting fission yeast gamma-tubulin complex function. *Mol Biol Cell* 15: 2287–2301
- Verollet C, Colombie N, Daubon T, Bourbon HM, Wright M, Raynaud-Messina B (2006) *Drosophila melanogaster* gamma-TuRC is dispensable for targeting gamma-tubulin to the centrosome and microtubule nucleation. *J Cell Biol* 172: 517–528
- Wainman A, Buster DW, Duncan T, Metz J, Ma A, Sharp D, Wakefield JG (2009) A new Augmin subunit, Msd1, demonstrates the importance of mitotic spindle-templated microtubule nucleation in the absence of functioning centrosomes. *Genes Dev* 23: 1876–1881
- Xiong Y, Oakley BR (2009) In vivo analysis of the functions of gamma-tubulin-complex proteins. *J Cell Sci* 122: 4218–4227
- Yanagawa S, Lee JS, Ishimoto A (1998) Identification and characterization of a novel line of *Drosophila* Schneider S2 cells that respond to wingless signaling. *J Biol Chem* 273: 32353–32359
- Yuba-Kubo A, Kubo A, Hata M, Tsukita S (2005) Gene knockout analysis of two gamma-tubulin isoforms in mice. *Dev Biol* 282: 361–373
- Zanic M, Widlund PO, Hyman AA, Howard J (2013) Synergy between XMAP215 and EB1 increases microtubule growth rates to physiological levels. *Nat Cell Biol* 15: 688–693
- Zheng YX, Jung MK, Oakley BR (1991) Gamma-tubulin is present in *Drosophila melanogaster* and *Homo sapiens* and is associated with the centrosome. *Cell* 65: 817–823
- Zhu H, Coppinger JA, Jang CY, Yates JR 3rd, Fang G (2008) FAM29A promotes microtubule amplification via recruitment of the NEDD1-gamma-tubulin complex to the mitotic spindle. *J Cell Biol* 183: 835–848
- Zimmerman S, Chang F (2005) Effects of  $\gamma$ -tubulin complex proteins on microtubule nucleation and catastrophe in fission yeast. *Mol Biol Cell* 16: 2719–2733